

## GALAXY EVOLUTION AND STAR FORMATION EFFICIENCY IN THE LAST HALF OF THE UNIVERSE

F. Combes<sup>1</sup>, S. García-Burillo<sup>2</sup>, J. Braine<sup>3</sup>, E. Schinnerer<sup>4</sup>, F. Walter<sup>4</sup>, L. Colina<sup>5</sup> and M. Gerin<sup>6</sup>

**Abstract.** We present the results of a CO(1-0) emission survey with the IRAM 30m of 30 galaxies at moderate redshift ( $z \sim 0.2-0.6$ ) to explore galaxy evolution and in particular the star formation efficiency, in the redshift range filling the gap between local and very high- $z$  objects. Our detection rate is about 50%. One of the bright objects was mapped at high resolution with the IRAM interferometer, and about 50% of the total emission found in the 27 arcsec (97 kpc) single dish beam is recovered by the interferometer, suggesting the presence of extended emission. The FIR-to-CO luminosity ratio is enhanced, following the increasing trend observed between local and high- $z$  ultra-luminous starbursts.

### 1 Introduction

It has been established that the star formation in the universe was one or two orders of magnitude larger in the past, had a maximum around  $z = 2$ , and then again faded towards zero beyond  $z = 6 - 8$  (e.g. Bouwens & Illingworth 2006). When the universe was half of its current age, at  $z = 0.7 - 0.8$ , the star formation rate was ten times larger than today. Observations also tend to show that the star forming objects were not the same, in the first half of the Hubble time. Starbursts occur first in the bigger galaxies, that are then quenched, while in the second half of the universe, star formation occurs in smaller objects, and this phenomenon is called downsizing.

This strong evolution of star-forming galaxies is not really understood, although it is suspected that galaxy interactions and mergers are certainly one of the main factors. The frequency of mergers with time has been estimated, through the perturbed morphologies, the asymmetry index and the number of galaxy pairs as a function of redshift. Luminous galaxies in particular, brighter than  $L_*$ , show a merger fraction of 10% at  $z = 1$ , and 50% at  $z = 3$  (Conselice 2006). Massive galaxies at  $z=3$  have 4-5 major mergers between  $z=3$  and 0, and most of them occur at  $z > 1.5$ .

This past active star formation in the universe contributes largely to the cosmic infrared background (CIB). About half of the galaxy formation and evolution escapes as direct starlight, the other half is re-radiated by dust. Galaxies contributing the most to the total CIB are  $z \sim 1$  luminous infrared galaxies, which have intermediate stellar masses (Dole et al 2006). The CIB has about the same brightness than the COB (the optical background), and both have only 5% of the brightness of the CMB. While today normal star forming galaxies dominate the star formation budget, the LIRGs begin to dominate beyond  $z=0.7$ , and the ULIRGs may be even earlier (e.g. Perez-Gonzalez et al. 2005).

To better understand the physics responsible for this evolution, it is essential to measure the molecular gas content of the intermediate redshift galaxies, and determine the Star Formation Efficiency (SFE), as a function of redshift. The SFE is estimated by the ratio of the far infrared luminosity (tracer of SF) to the CO emission

---

<sup>1</sup> Observatoire de Paris, LERMA (CNRS:UMR8112), 61 Av. de l'Observatoire, 75014 Paris, France

<sup>2</sup> Observatorio Astronómico Nacional (OAN)-Observatorio de Madrid, Alfonso XII, 3, 28014-Madrid, Spain

<sup>3</sup> Observatoire de Bordeaux, Université Bordeaux I, BP 89, 33270 Floirac, France

<sup>4</sup> Max-Planck-Institut für Astronomie (MPIA), Königstuhl 17, 69117 Heidelberg, Germany

<sup>5</sup> IEM, Consejo Superior de Investigaciones Científicas (CSIC), Serrano 121, 28006 Madrid, Spain

<sup>6</sup> Radioastronomie ENS, 24 Rue Lhomond, 75005 Paris, France

(tracer of the  $H_2$  content). This efficiency appears to increase with redshift, at least for objects detected. For instance the Submillimeter Galaxies (SMGs), are apparently more efficiently forming stars than ULIRGs, with SFR of  $\sim 700 M_\odot/\text{yr}$ , during a starbursting phase of 40- 200 Myr (Greve et al 2005). A possibility is that these early objects have not yet accumulated bulges, and mergers without bulges could be more violently active.

## 2 Observation of 30 ULIRGs at intermediate $z$

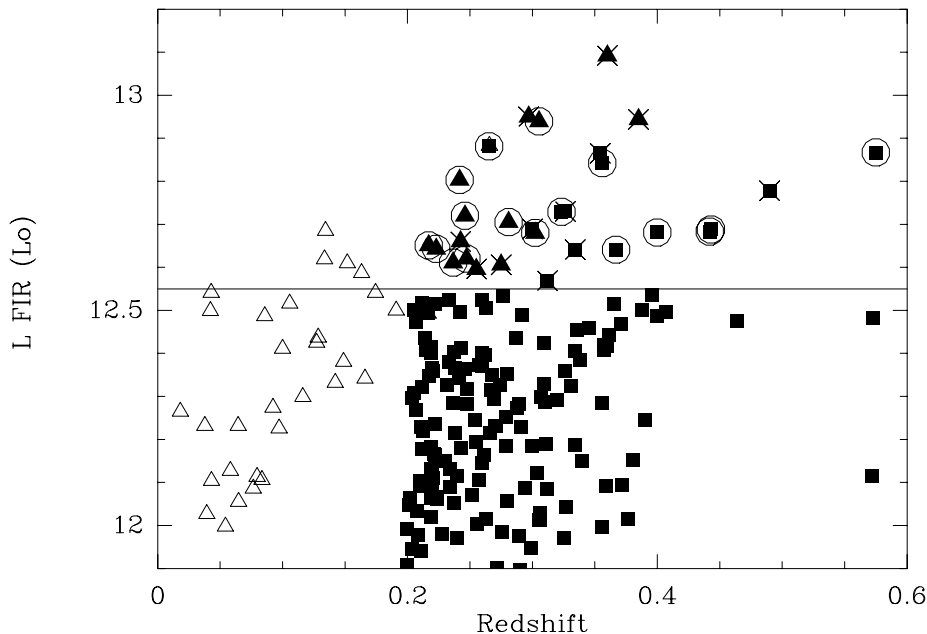


**Fig. 1.** Plot of far-infrared luminosity,  $L_{\text{FIR}}$ , of ULIRGs as a function of redshift,  $z$ , in the local sample of Solomon et al. (1997) (open triangles) and our sample (filled symbols). We have observed at the IRAM-30m the points above the horizontal line (30 sources). The circles indicate secure detections, non-detections are marked by a cross.

Up to now, very little is known about the molecular gas content of galaxies at moderate redshift. The local ULIRGs sample of Solomon et al (1997) contains 37 objects, but only 2 have redshifts of  $z > 0.2$ . We have undertaken a systematic survey of  $0.2 < z < 0.6$  sources, to begin to fill the gap between low- $z$  and high- $z$  ( $> 2$ ) studies. We have selected all objects (209 galaxies) at declinations greater than  $-12^\circ$  with spectroscopic redshifts and a detected 60 micron flux (from IRAS or ISO). Most of the galaxies (and in particular the brightest ones) have also detailed photometry in the NIR bands, from the samples by Clements et al (1996), Kim & Sanders (1998), Kim et al (2002) and Stanford et al (2000). The optical spectroscopy shows that no signs of AGN features are present in their spectra. According to their sub-arcsec K-band images (see ref above), about two-thirds of the objects are interacting galaxies.

We observed the 30 brightest IR-luminous objects (cf Fig 1). Among them, 17 were detected (Combes et al, in prep). The  $H_2$  masses were derived from the CO emission, using a conversion factor which is 5 times lower than the standard one, as advocated by Solomon et al (1997) to be applied to ULIRGs. Fig 2 then compares the far infrared luminosities with  $H_2$  masses, to estimate star formation efficiencies. The detected objects have in general high SFE with respect to the more local sample (for which the same conversion ratio was used). In addition to dynamical processes being more efficient in star formation, another possible explanation to this high SFE measured by  $L_{\text{FIR}}/M(H_2)$  could be partly due to a non negligible AGN contribution to the FIR luminosity. Although we excluded in the sample the possible AGN (no-identification in optical spectra), there still might be some highly embedded/obscured AGNs. It has been established that the fraction of AGNs in ULIRGs rapidly increases with the luminosity above  $\log(L/L_\odot) \sim 12.5$  (e.g. Tran et al. 2001).

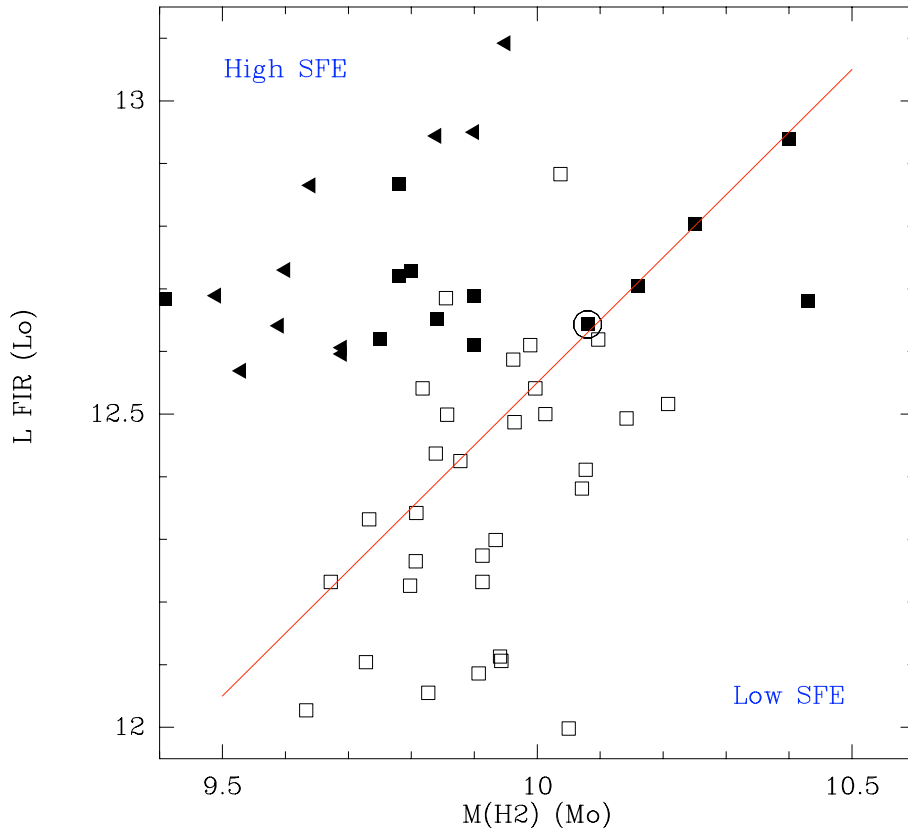


**Fig. 2.** In this plot of  $L_{\text{FIR}}$  versus  $M(\text{H}_2)$ , the local sample from Solomon et al. (1997) is again indicated as open symbols, while our observed galaxies are filled symbols. Upper limits are indicated as triangles and squares are detections. The diagram helps to identify the high star formation efficiency (SFE) objects in the upper left, and low SFE in the lower right. Note the high SFE of our sample. The galaxy observed with the IRAM interferometer is indicated by a circle.

### 3 Mapping of one of the ULIRGs at $z=0.223$

We mapped with the Plateau de Bure interferometer one of the best-detected galaxies, IRAS 11582+3020. It is an ultra-luminous galaxy with  $L(\text{IR}) = 5.4 \cdot 10^{12} L_{\odot}$ , classified as a LINER by Kim et al. (1998). Rupke et al. (2005) find evidence of a superwind outflow in this galaxy of about  $15 M_{\odot} \text{yr}^{-1}$ , while its SFR is estimated at  $740 M_{\odot} \text{yr}^{-1}$  from the infrared luminosity. The red image of Kim et al. (2002) reveals some extended diffuse emission, which could be diluted tidal tails, from a recent interaction, while two galaxies of the same group are within 90 kpc in projection (Fig 3).

IRAS 11582+3020 was observed in CO(1–0) first with the IRAM-30m, with a beam of  $27''$  ( $= 97$  kpc) at a frequency of 94.25 GHz, and then with the Plateau de Bure Interferometer (PdBI), with a beam of  $1.3'' \times 1.0''$ . No continuum emission was detected at 3mm (possible AGN) or at 1mm (possible dust emission), down to rms noise levels of  $0.1 \text{ mJy beam}^{-1}$  and  $0.5 \text{ mJy beam}^{-1}$ . Given the IRAS  $100\mu\text{m}$  flux of 1.5 Jy, the upper limit at 1.2mm is compatible with a typical starburst SED.

The single dish and interferometer spectra are compared in Fig 3. The PdBI flux is only  $\sim 50\%$  of the 30m flux, suggesting extended emission beyond  $10''$  (36kpc), which is consistent with the extended optical structure, and hints at a weak diffuse tidal tail in this perturbed system. The  $\text{H}_2$  mass derived from the 30m spectrum is  $1.2 \cdot 10^{10} M_{\odot}$ , and  $6 \cdot 10^9 M_{\odot}$  with the PdBI (with the low conversion factor used for ULIRGs).

The integrated CO(1–0) map is plotted in Fig 4, together with the red and blue channel maps. The source is resolved at least in the direction of the beam's minor axis, where the deconvolved size of the CO emitting region is of the order of  $0.8''$ , in diameter ( $\sim 3$  kpc). It is possible to detect the shift of the barycenter in each channel map, with a kinematic major axis aligned at  $\text{PA} \sim 135^\circ$  (Fig 5). Since  $\sim 135^\circ$  is also the position angle

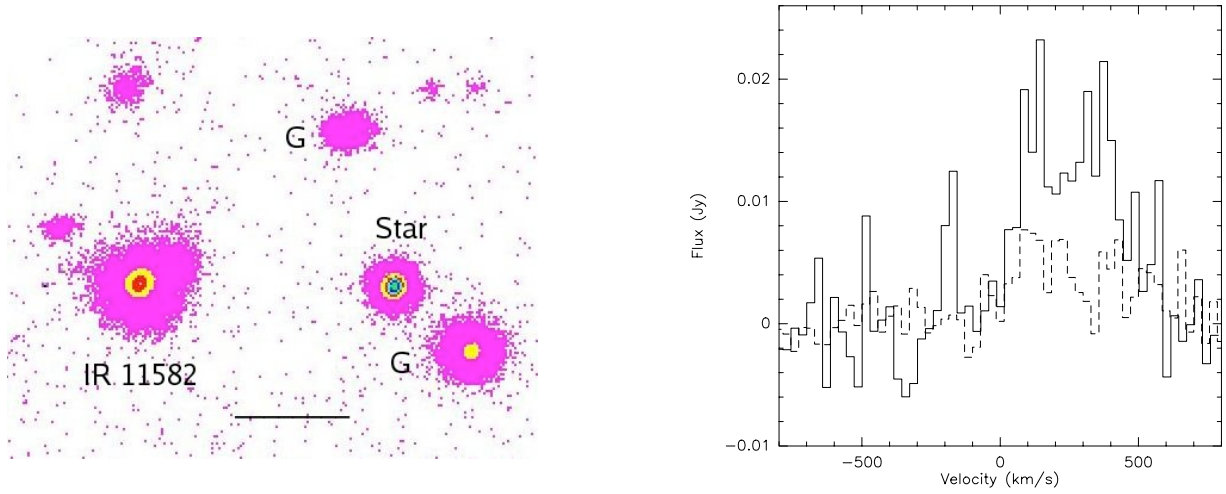


**Fig. 3.** **Left:** Red image of IRAS 11582+3020 from Kim et al. (2002). The two objects marked "G" are galaxies in the same group (a foreground star is also indicated). The length of the horizontal bar at the bottom is 10 arcsec = 36 kpc at  $z=0.223$ . **Right:** The IRAM 30m CO(1-0) spectrum (solid line), compared with the integrated spectrum from the interferometer (dashed line). The velocity is relative to  $z=0.223$  (from Combes et al 2006).

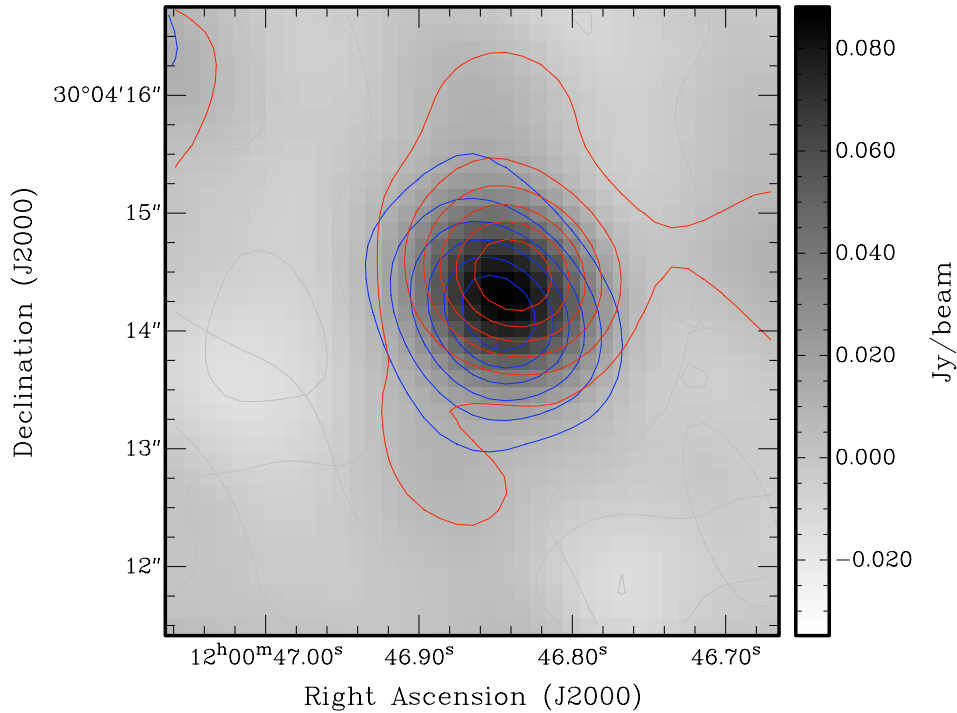


**Fig. 4.** Blue and red velocity channels superposed on the CO(1-0) image of IRAS 11582+3020, obtained with the Plateau de Bure interferometer. A gradient of velocity is apparent.

of the extended optical isophotes (Fig 3), all available data are compatible with a post-merger relaxed system. The estimated dynamical mass is  $M_{dyn} = 3.4 \cdot 10^{10} M_{\odot}$ .

In summary, the CO emission in IRAS 11582+3020 suggests the presence of two components: a nuclear disk 1.5kpc in radius with a nuclear starburst (as usual in local starbursting galaxies, where disks of radii= 300-800pc are found, Downes & Solomon 1998); and a more extended disk up to 20-30kpc diameter, which

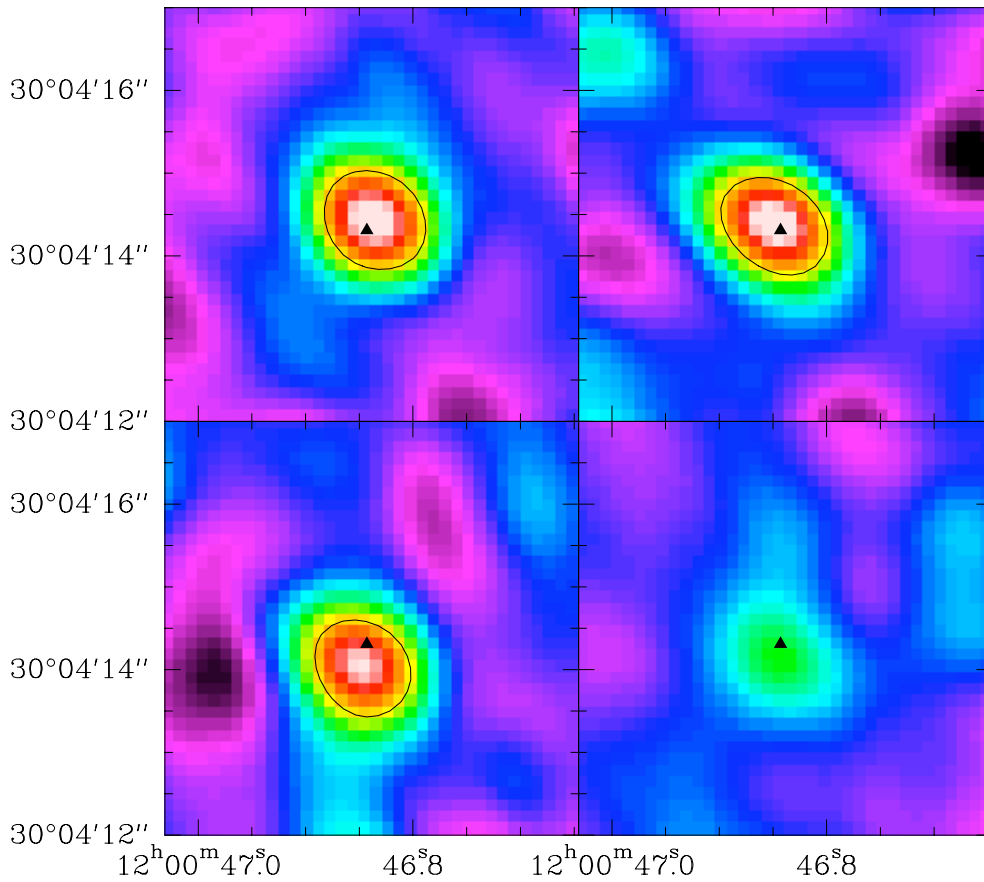


**Fig. 5.** Four equidistant channel maps of IRAS 11582+3020, from 500 to 0 km/s (top left to bottom right), showing the barycenter moving along a position angle of  $\sim 135^\circ$ .

would correspond to the optical merger morphology.

The physical properties of IRAS 11582+3020 (size, SFE) appear to be intermediate between those of local ULIRGs and high- $z$  submillimeter galaxies (SMG) as mapped by Tacconi et al. (2006). There might be a trend, also followed by IRAS 11582+3020, for high- $z$  galaxies to have a higher  $L(\text{FIR})/M(\text{H}_2)$  ratio (Riechers et al. 2006), however this must be confirmed with larger samples.

#### 4 Problems and perspectives

To tackle galaxy evolution, and the star formation efficiency as a function of redshift, one of the main problem beyond sensitivity is the identification of submillimeter sources detected in continuum (only 5-10% are identified). Surveys carried out in the far infrared suffer from confusion (Spitzer, ASTRO-F, Herschel). The contribution of AGN to the infrared luminosity has to be determined. In the future, the redshift of the sources could be obtained directly from molecular lines ("redshift machine" on LMT, GBT, CCAT, ALMA...).

In particular, with a spatial resolution  $< 0.1''$ , there will be no confusion with ALMA. Its sensitivity will allow the detection of non ULIRGs and more "normal" galaxies, for example Lyman-Break Galaxies (Steidel et al 1996, Adelberger & Steidel 2000), which are observed optically with a density of 150/arcmin<sup>2</sup> at  $z=2.5-3.5$ . There will be a complement to MUSE on the VLT, providing large samples of Lyman- $\alpha$  emitters.

We wish to thank the IRAM staff for help with the observations, both at the 30m and Plateau de Bure interferometer. IRAM is supported by INSU/CNRS (France), MPG (Germany), and IGN (Spain).

## References

- Adelberger K.L., Steidel C.C.: 2000, ApJ 544, 218
- Bouwens R. J., Illingworth G.D.: 2006, Nature 443, 189B
- Clements, D., Sutherland, W. Saunders, W. et al: 1996, MNRAS 279, 459 & 477
- Combes F., Garcia-Burillo, S., Braine, J. et al.: 2006, A&A 460, L49
- Conselice C.J.: 2006, in ESO Astrophysics Symposia: "Groups of Galaxies in the Nearby Universe", eds. I. Saviane, V. Ivanov, J. Borissova
- Dole H., Lagache G., Puget J.-L. et al.: 2006, A&A 451, 417
- Downes D., Solomon P.: 1998, ApJ 507, 615
- Greve, T. R., Bertoldi, F., Smail, I. et al.: 2005, MNRAS 359, 1165
- Kim D.C., Sanders D.B.: 1998, ApJS 119, 41
- Kim D.C., Veilleux S., Sanders D.B.: 2002, ApJS 143, 277
- Perez-Gonzalez P. G., Rieke, George H., Egami, E. et al.: 2005 ApJ 630, 82
- Riechers, D.A., Walter, F., Carilli, C. et al.: 2006, AJ, 650, 604
- Rupke D.S., Veilleux S., Sanders D.B.: 2005 ApJS 160, 115
- Solomon P., Downes D., Radford S., Barrett J.: 1997, ApJ 478, 144
- Stanford S.A., Stern D., van Breugel W., de Breuck C.: 2000 ApJS 131, 185
- Steidel C.C., Gialalisco, M., Dickinson, M., Adelberger, K. L.: 1996, AJ 112, 352
- Tacconi L.J., Neri R., Chapman S.C. et al.: 2006, ApJ 640, 228
- Tran Q. D., Lutz, D., Genzel, R. et al. 2001 ApJ 552, 527